

Interface properties of NiMnSb/InP and NiMnSb/GaAs contacts

Iosif Galanakis,* Marjana Ležaić, Gustav Bihlmayer, and Stefan Blügel

Institut für Festkörperforschung, Forschungszentrum Jülich, D-52425 Jülich, Germany

(Received 13 September 2004; revised manuscript received 20 December 2004; published 30 June 2005)

We study the electronic and magnetic properties of the interfaces between the half-metallic Heusler alloy NiMnSb and the binary semiconductors InP and GaAs using two different state-of-the-art full-potential *ab initio* electronic structure methods. Although in the case of most NiMnSb/InP(001) contacts the half-metallicity is lost, it is possible to keep a high degree of spin polarization when the interface is made up by Ni and P layers. In the case of the GaAs semiconductor, the larger hybridization between the Ni-*d* and As-*p* orbitals with respect to the hybridization between the Ni-*d* and P-*p* orbitals destroys this polarization. The (111) interfaces present strong interface states, but also in this case there are few interfaces presenting a high spin polarization at the Fermi level which can reach values up to 74%.

DOI: 10.1103/PhysRevB.71.214431

PACS number(s): 75.47.Np, 73.20.At, 71.20.Lp

I. INTRODUCTION

The spin injection from a metal into a semiconductor remains one of the main challenges in the field of magnetoelectronics.¹⁻³ The use of half-metallic ferromagnets as electrodes was proposed to maximize the efficiency of spintronic devices. These compounds are ferromagnetic metals with a band gap at the Fermi level (E_F) for the minority spin band leading to 100% spin polarization at E_F . But even in this case, interface states at the contact between the half-metal and the semiconductor can destroy the half-metallicity. Due to their orthogonality to all bulk states incident to the interface, in the ballistic limit these states should not affect the transport properties, but it is their interaction with other defect states which makes them conducting.

The first material predicted to be a half-metal is the Heusler alloy NiMnSb.⁴ There exist several *ab initio* calculations on NiMnSb reproducing the initial results of de Groot and collaborators,⁵⁻⁹ and Galanakis *et al.* showed that the gap arises from the hybridization between the *d* orbitals of the Ni and Mn atoms.¹⁰ Experiments seem to well establish its half-metallicity in the case of single crystals,^{11,12} but in films the half-metallicity is lost.¹³⁻²¹ Theoretical calculations for the interfaces of these materials with semiconductors are few and all results agree that in general the half-metallicity is lost at the interface between the Heusler alloy and the semiconductor.²²⁻²⁶ Wijs and de Groot have argued that in the case of the NiMnSb/CdS(111) contacts the Sb/S interface keeps half-metallicity when the S atoms sit exactly on top of Sb.²² Thus, it is possible that a high degree of spin polarization stays at the interface and these structures remain attractive for realistic applications.

We should also mention that even in the absence of the interface states, true half-metallicity cannot really exist due to minority states induced by the spin-orbit coupling which couples the two spin bands. But as it was shown for these systems in Refs. 27 and 28, this phenomenon is very weak and instead of a gap in the minority channel there is a region of still almost 100% spin polarization. It was also found that the orbital moments are very small in these compounds.²⁹ Thus, spin-orbit coupling can be assumed to be negligible with respect to the interface states.

The aim of this study is to identify interfaces where the spin polarization at the Fermi level is very high. In real experiments, the interface is difficult to be controlled and in most cases reconstructions and interdiffusion lead to complicated interfaces which are difficult to simulate in first-principles calculations. A study of ideal low-index interfaces between a half-metallic system and a semiconductor—as the one presented here—can identify some ideal cases of high spin polarization. Thereby, it can stimulate further experimental work to prepare similar interfaces by controlling the growth conditions of the samples. We should note here that in the case of spin-injection experiments, the detection of the spin current is a very difficult task.^{30,31} The presence of defects and disorder at the interface, even at a small percentage, would completely suppress small values of spin polarization. In these experiments, only cases where the spin polarization at the Fermi level exceeds 70% and more than 90% of electrons at the Fermi level are of majority-spin character are really interesting for practical applications.

In this communication, we study the (001) interfaces of the half-metallic NiMnSb Heusler alloy with InP and GaAs and the (111) interface between the NiMnSb and InP compounds. We take into account all possible contacts and show that there are cases where a high degree of spin polarization remains at the interface. In Sec. II we discuss the structure of the interfaces and the computational details, and in Sec. III we present and analyze our results for the (001) interfaces. In Sec. IV we discuss the (111) interfaces, and finally in Sec. V we summarize and conclude.

II. COMPUTATIONAL METHOD AND STRUCTURE

In the calculations, we used two different full-potential methods. First, we employed the full-potential version of the screened Korringa-Kohn-Rostoker (FSKKR) Green's-function method^{32,33} in conjunction with the local-spin-density approximation (LDA)³⁴ to the density-functional theory^{35,36} to study the (001) interfaces between NiMnSb and the InP and GaAs semiconductors. The FSKKR method scales linearly with the number of atoms and, therefore, allows us to study also very thick slabs of these materials. But

it cannot give exactly the Fermi level of semiconductors due to problems arising from the ℓ_{\max} cutoff in this method³⁷ and, thus, we employed also the full-potential linearized augmented-plane-wave method (FLAPW)^{38,39} in the FLEUR implementation⁴⁰ to calculate the NiMnSb/InP(001) interfaces in order to compute the band offset. Finally, the FLAPW method was also employed in the case of the NiMnSb/InP(111) interfaces.

NiMnSb crystallizes in the $C1_b$ structure, which consists of four interpenetrating fcc sublattices. The unit cell is that of a fcc lattice with four atoms as basis at $A=(000)$, $B=(\frac{1}{4}\frac{1}{4}\frac{1}{4})$, $C=(\frac{1}{2}\frac{1}{2}\frac{1}{2})$, and $D=(\frac{3}{4}\frac{3}{4}\frac{3}{4})$ in Wyckoff coordinates.¹⁰ In the case of NiMnSb, the A site is occupied by Ni, the B site by Mn, and the D site by Sb, while the C site is unoccupied. The $C1_b$ structure is similar to the $L2_1$ structure adopted by the full Heusler alloys, like Ni_2MnSb , where also the C site is occupied by a Ni atom.⁴¹ The zincblende structure, adopted by a large number of semiconductors like GaAs and InP, can also be considered as consisting of four fcc sublattices. In the case of GaAs, the A site is occupied by a Ga atom, the B site by an As atom, while the C and D sites are empty. Depending on the electronic structure method used to perform the calculations, one either uses empty spheres or empty polyhedra to account for the vacant sites (as is done in the FSKKR) or the vacant sites just make part of the interstitial region (as in the FLAPW). Within 1% accuracy, NiMnSb (5.91 Å) has the same experimental lattice constant as InP (5.87 Å) and epitaxial growth of NiMnSb on top of InP has been already achieved experimentally by molecular-beam epitaxy.^{13,14} On the other hand, the lattice constant of GaAs (5.65 Å) is almost 4% smaller. The dominant effect at the interface is the expansion or the contraction of the lattice of the half metal along the growth axis to account for the in-plane change of its lattice parameter.^{23–25} Since in the case of the NiMnSb/InP interface both compounds have similar lattice parameters, in the calculations perfect epitaxy can be assumed.

Within the FSKKR, the space is divided into nonoverlapping Wigner-Seitz polyhedra and thus empty ones are needed to describe accurately the vacant sites (similarly to the use of empty spheres in the early electronic structure methods). To simulate the (001) interface within the FSKKR calculations, we used a multilayer consisting of 15 layers of the half-metal and 9 semiconductor layers. This thickness is enough so that the layers in the middle of both the half-metallic part and the semiconducting one exhibit bulk properties. There are several combinations at the interface, e.g., at the NiMnSb/InP contact the interface can be either a Ni/In one, Ni/P, MnSb/In, or MnSb/P (see Fig. 1). We will keep this definition throughout the paper to denote different interfaces. We should also mention that since the multilayer contains 15 half-metal and 9 semiconductor layers, there are two equivalent surfaces at both sides of the half-metallic spacer. Finally, for our FSKKR calculations we used a $20 \times 20 \times 4$ grid in the \mathbf{k} space and we took into account wave functions up to $\ell_{\max}=3$ and thus the potential and the charge density were expanded on lattice harmonics up to $\ell_{\max}=6$. All FSKKR calculations have been performed at the experimental lattice constant of NiMnSb (5.91 Å).

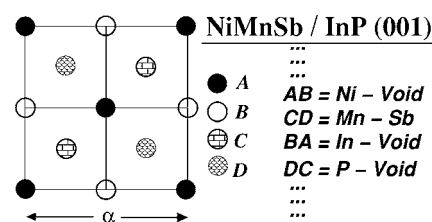


FIG. 1. Schematic representation of the (001) interface between NiMnSb and InP. There are several different combinations at the interface which can be either Ni/In, Ni/P, MnSb/In (shown in the figure), or MnSb/P.

In the FLAPW method, the space is divided into nonoverlapping muffin-tin spheres around each atom and an interstitial region that is described in terms of plane waves. To perform the calculations for the (001) interfaces, we employed a repeated slab made up of eight layers of NiMnSb and eight layers of the semiconductor. Thus if the one contact is Ni/P, the other one is MnSb/In. As will be shown in Sec. III C, the smaller number of layers (as compared to the FSKKR calculations) does not influence the properties near the Fermi level. For the (111) interfaces, the supercells consisted of 16 layers of NiMnSb and 12 layers of InP. The FLAPW calculations were performed using density-functional theory in the generalized gradient approximation (GGA) as given by Perdew *et al.*⁴² For the calculations, a plane-wave cutoff K_{\max} of 3.45 a.u.^{-1} was used. Lattice harmonics with angular momentum $l \leq 8$ were used to expand the charge density and the wave functions within the muffin-tin spheres, having a radius of 2.4 a.u. for Sb and 2.34 a.u. for all the other atoms. The Brillouin zone (BZ) was sampled with 128 special \mathbf{k} points in the irreducible wedge (1/8 of the whole BZ) for (001) interfaces, and 90 \mathbf{k} points in the irreducible wedge (1/12 of the whole BZ) for the (111) interfaces. All FLAPW calculations were performed at the experimental lattice constant of InP (5.87 Å) except for these cases, where the relaxation effects at the interfaces have been checked. There, the theoretically optimized lattice constant of InP (5.94 Å) has been used.

III. NiMnSb/InP AND NiMnSb/GaAs (001) INTERFACES

Compared to simple surfaces, interfaces are more complex systems due to the hybridization between the orbitals of the atoms of the metallic alloy and the semiconductor at the interface. Thus, results obtained for the surfaces (as the ones in Refs. 43–46) cannot be easily generalized for interfaces since for different semiconductors different phenomena can occur. In both (001) and (111) surfaces of NiMnSb, the appearance of surface states destroys the half-metallicity.^{43,44} In Secs. III A and III B, we present the FSKKR results for the NiMnSb/InP(001) and NiMnSb/GaAs(001) contacts, respectively, and in Sec. III C we give the valence-band offsets calculated with the FLAPW method for the NiMnSb/InP(001) interfaces and compare the results obtained with the two different methods.

A. NiMnSb/InP contacts

The first case which we will study are the interfaces between NiMnSb and InP. In Table I we have gathered the

TABLE I. FSKKR-calculated atomic spin moments given in μ_B for the interface between the MnSb-terminated (001) NiMnSb and the In- or the P-terminated InP. We do not present the spin moments at the vacant sites. The last columns are the moments for the MnSb-terminated NiMnSb(001) surface and the bulk NiMnSb. “I” denotes the interface layers and \pm means one layer deeper in the half-metal or the semiconductor.

	MnSb/In	MnSb/P	MnSb surf.	Bulk
I-3	Ni: 0.270	Ni: 0.275	Ni: 0.269	Ni: 0.264
I-2	Mn: 3.704	Mn: 3.734	Mn: 3.674	Mn: 3.705
I-2	Sb: -0.057	Sb: -0.044	Sb: -0.066	Sb: -0.062
I-1	Ni: 0.289	Ni: 0.316	Ni: 0.223	Ni: 0.264
I	Mn: 3.405	Mn: 3.718	Mn: 4.018	Mn: 3.705
I	Sb: -0.037	Sb: -0.045	Sb: -0.096	Sb: -0.062
I	In: -0.053	P: 0.015		
I+1	P: -0.022	In: -0.013		
I+2	In: -0.017	P: -0.011		
I+3	P: -0.012	In: 0.002		

FSKKR spin moments for the case of the MnSb/In and MnSb/P interfaces. “I” stands for the interface layers, +1 means moving one layer deeper in the semiconductor, and -1 one layer deeper in the half-metallic spacer. In the case of the MnSb terminated half-metallic film, there is a difference depending on the semiconductor termination. In the case of the In termination, the Mn spin moment decreases considerably and is now $3.4\mu_B$ compared to the bulk value of $3.7\mu_B$. For the P-terminated InP film, the spin moment of Mn at the interface is very close to the bulk value. In the case of the bulk NiMnSb, the minority gap is created by the hybridization between the d orbitals of the Ni and Mn atoms, but the Sb atom plays also a crucial role since it provides states lower in energy than the d bands which accommodate electrons of the transition-metal atoms.¹⁰ Moreover, Mn and Ni atoms create a common majority band where there is a charge transfer from the Mn atoms towards the Ni ones. On the MnSb-terminated surface, each Mn atom loses two out of its four nearest Ni atoms and regains this charge which fills up mainly majority states. The Mn spin moment at the surface is strongly enhanced reaching $4.0\mu_B$. In the case of the interfaces, the final spin moment of the Mn atom at the interface depends on the hybridization with the neighboring atoms of the semiconductor. At an In interface, the Mn minority d states hybridize strongly with the In states and thus the Mn spin moment is severely reduced and In shows a negative induced spin moment. In the case of P, the situation is reversed and P has a positive induced spin moment. The Mn- d -P- p hybridization is not as strong as the Mn- d -In- p one and the Mn spin moment at the interface is close to the bulk value. We should also note that, if we move deeper into the half-metallic film, the spin moments regain their bulklike behavior while, if we move deeper in the semiconductor film, the induced spin moments quickly vanish.

On a MnSb-terminated (001) surface, the spin polarization at the Fermi level, E_F , was found to be as high as 38% [the spin polarization is defined with respect to the density of states $n(E)$,

$$P = \frac{n^\uparrow(E_F) - n^\downarrow(E_F)}{n^\uparrow(E_F) + n^\downarrow(E_F)},$$

where \uparrow stands for the majority electrons and \downarrow for the minority electrons]. In Ref. 45, two surface states at E_F were reported to destroy the half-metallicity, but still the population of the majority electrons at the Fermi level was twice as large as the one of the minority states. Compared to this surface, for the interfaces between MnSb-terminated NiMnSb and InP the situation is completely different. The hybridization between the d states of Mn and p states of Sb with the p states of either the In or the P atom at the interface is such that the net polarization at the interface is almost zero. This is clearly seen in Fig. 2, where we present with the dashed line the spin- and atom-resolved density of states (DOS) of the atoms at the interface for a MnSb/P contact. There is a minority interface state pinned at the Fermi level which destroys the half-metallicity. In the Mn local DOS, this state overlaps with the unoccupied minority Mn states and it is not easily distinguished but its existence is obvious if one examines the Ni and Sb DOS. The situation is similar also for the MnSb/In contact not shown here.

In the case of the Ni-terminated NiMnSb films, the DOS at E_F is more bulklike than the case of the MnSb films. Already the Ni interface atom has a spin moment of $0.29\mu_B$ in the case of an interface with In and $0.36\mu_B$ for an interface with P compared to the bulk value of $0.26\mu_B$. In the bulk case, Ni has four Mn and four Sb atoms as first neighbors. On the Ni-terminated (001) surface, the Ni atom loses half of its first neighbors. But if an interface with P is formed, the two lost Sb neighbors are replaced by two isovalent P atoms and—with the exception of the Mn neighbors—the situation is very similar to the bulk. Now the Sb p bands at lower energy are not destroyed since P has a behavior similar to Sb and still they accommodate three transition-metal d electrons. Thus the only change in the DOS comes from the missing two Mn neighboring atoms. The DOS in Fig. 2 for the Ni/P case is clearly very close to the bulk case and in

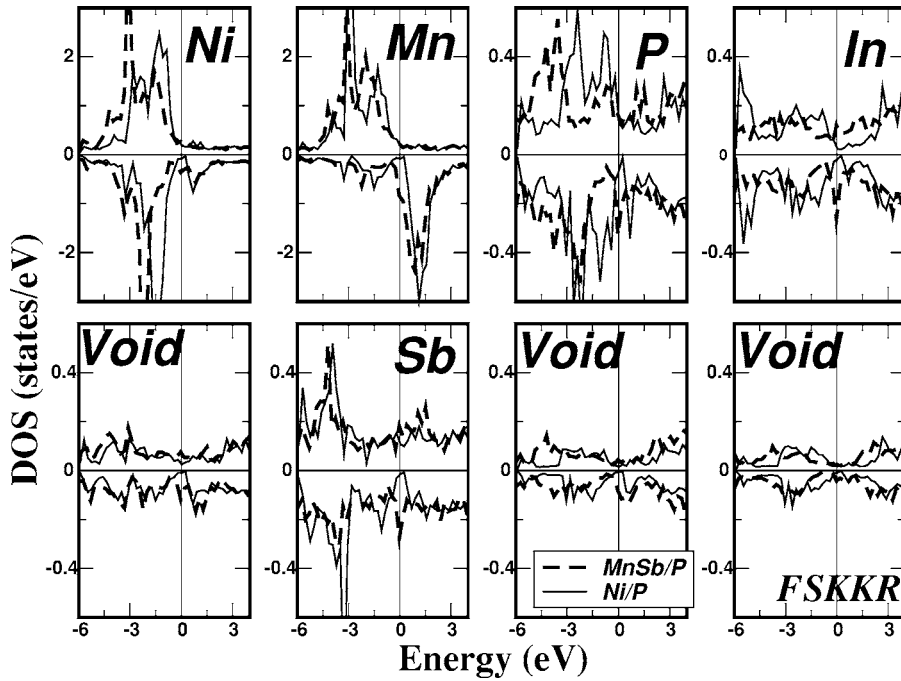


FIG. 2. Atom- and spin-resolved DOS for the case of MnSb/P (dashed line) and Ni/P (solid line) contacts for the two interface layers and one layer deeper in the half-metal and the semiconductor. The zero of the energy is chosen to correspond to the Fermi level. Positive values of the DOS correspond to the majority spin and negative to the minority.

Fig. 3 we have gathered the DOS for the Ni and the void at the interface and the Mn and Sb atoms at the subinterface layer for both Ni/In (dashed line) and Ni/P (solid line) contacts and we compare them with the bulk results from Ref. 10. In the case of the Ni/In interface, there is an interface state pinned at the Fermi level which completely suppresses the spin polarization P (if we take into account the first two interface layers then $P \approx 0$). In the case of the Ni/P interface, the intensity of these interface states is strongly reduced and now the spin polarization for the first two interface layers is 39%, i.e., about 70% of the electrons at the Fermi level are of majority spin character.

It should be noted here that all given data up to this point refer to unrelaxed interfaces. Relaxation effects modify these values: Increased hybridization and charge transfer can lead to pronouncedly reduced spin polarizations at the interface. The Ni-P interlayer distance is reduced by 18%, while the

neighboring interlayer distances are expanded by 5–7% as compared to the ideal bulk values. Thereby, the spin polarization at the interface is decreased to only 17%. Nevertheless, these effects do not destroy the gap completely, they just lead to a shift of the local DOS and can be compensated by a doping of the interface. We found that substituting one-third of the Ni atoms by Cu increases the spin polarization at the interface again to 55%.

B. NiMnSb/GaAs contacts

In the previous section, it was shown that in the case of the Ni/P interfaces the spin polarization was as high as 39%. In order to investigate whether this is a general result for all semiconductors or specifically for this interface, we also performed calculations for the case of the NiMnSb/GaAs(001) contacts using the same lattice parameter as for the previous

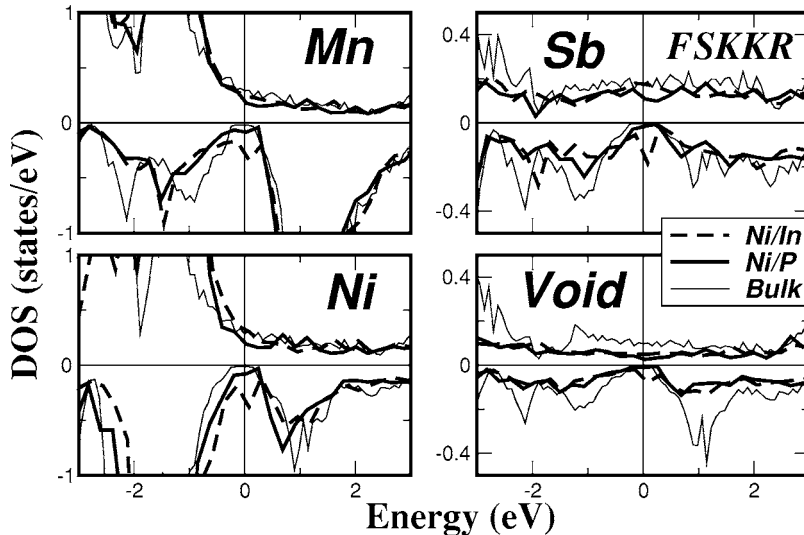


FIG. 3. Bottom: Spin- and atom-resolved DOS for the Ni and “Void” atoms at the interface with In (dashed line) or P (solid line). The top panels show the Mn and Sb DOS at the subinterface layer. The thin solid line indicates the results for bulk NiMnSb from Ref. 10.

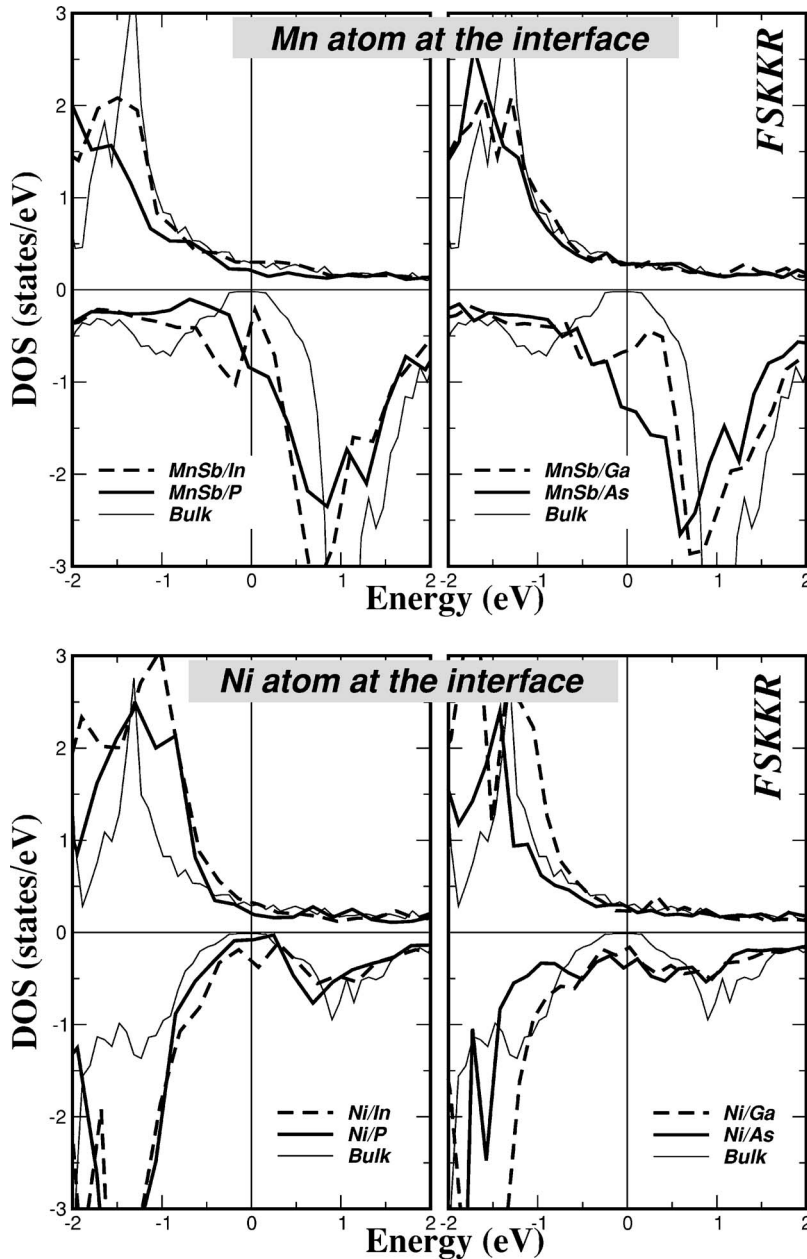


FIG. 4. Left-top panel: atom- and spin-resolved DOS for the case of MnSb/In (dashed line) and MnSb/P (solid line) contacts for the Mn atom at the interface layer. Right-top panel: similar results for the MnSb/Ga and MnSb/As contacts. Bottom panels contain the results for the Ni-terminated half-metallic spacer. With the thin solid line, the bulk results are indicated.

ones; thus the lattice constant of GaAs was expanded by approximately 4%. From the experimental point of view, it is the Heusler alloy which grows on top of the semiconductor substrate and thus normally the NiMnSb lattice constant should change to match the semiconductor and not the opposite. Our choice to expand the GaAs lattice constant was motivated by the fact that in this case the results can be directly compared with the NiMnSb/InP junction.

In the top panel of Fig. 4, the atom-resolved DOS for the Mn at the interface layer is shown for the case of the MnSb/semiconductor interfaces. The hybridization between the d orbitals of the Mn atom at the interface and the p orbitals of the sp atoms of the semiconductor is larger in the case of the GaAs than for the InP spacer. This leads to about $0.1-0.2\mu_B$ smaller Mn spin moments at the interface, and the exchange splitting between the occupied Mn majority and the unoccupied Mn minority d states is smaller. Thus the large minority

peak above the Fermi level moves lower in energy and now strongly overlaps with the occupied minority peak below the Fermi level increasing the minority DOS at the Fermi level. In the meantime, the smaller exchange splitting causes the shift of the occupied Mn majority states towards higher energies enhancing also the Mn majority DOS at the Fermi level. The final spin polarization at the Fermi level in the case of the MnSb/Ga or As contacts is similar to the MnSb/In and MnSb/P ones and these interfaces are not interesting for real applications.

The same effect occurring for the MnSb interface can also be seen at the Ni interfaces, as shown in the bottom panels of Fig. 4. The stronger hybridization of the Ni atom with either the Ga or As atoms at the interface with respect to the InP semiconductor provokes a movement of the Ni unoccupied minority d states towards lower energies while the occupied majority ones are moving higher in energy. If one looks in

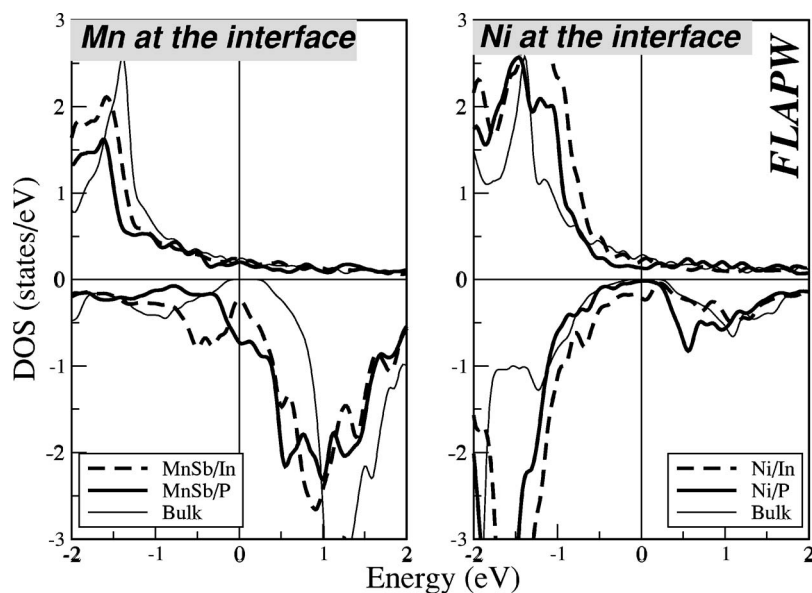


FIG. 5. Left panel: atom- and spin-resolved DOS for the case of MnSb/In(001) (dashed line) and MnSb/P(001) (solid line) contacts for the Mn atom at the interface layer as calculated with the FLAPW method. Right panel: results for the Ni atom at the Ni/In and Ni/P interface for the Ni-terminated half-metallic spacers. The thin solid line indicates the local DOS of bulk NiMnSb.

detail at the Ni/In and Ni/Ga contacts, one observes that the minority peak at the Fermi level present in the Ni/In contact is now smeared out in the case of the Ni/Ga contact due to the unoccupied minority states which move lower in energy. Similarly, the unoccupied Ni minority d states have a larger bandwidth in the case of the Ni/As contact than in the case of the Ni/P one inducing a high minority Ni DOS at the Fermi level. The high spin polarization at the Fermi level presented in the case of the Ni/P interfaces is completely destroyed in the case of the Ni/As contact due to the larger hybridization between the Ni- d and As- p orbitals with respect to the hybridization between the Ni- d and P- p orbitals. Thus, the properties of the interface depend also in a large extent on the choice of the semiconductor.

C. Band offsets and partial DOS for NiMnSb/InP contacts

Employing the FLAPW method, we calculated the (minority states) valence-band offset which is the energy difference between the maximum of the valence band (VBM) of the semiconductor and the maximum of the minority valence band of the Heusler alloy. To calculate it, we referenced the binding energies of the core states in the interface calculation to their corresponding bulk values as described in Ref. 47. We found that the VBM of the semiconductor is 0.83 eV lower than the one of the half-metal for the In/MnSb contact. For the other interfaces, the valence-band offsets are 0.69 eV for the In/Ni, 0.69 for the P/Ni, and 0.80 eV for the P/MnSb contact. In the bulk InP semiconductor, the experimental gap is 1.6 eV, thus the Fermi level, which is 0.07 eV above the maximum of the minority NiMnSb valence band, falls in the middle of the semiconductor bulk band gap. This is similar to what is happening also in the case of the $\text{Co}_2\text{MnGe}/\text{GaAs}$ (001) interfaces²⁴ and these junctions can be used to inject spin-polarized electrons in the semiconductor.

We can now also compare the results obtained with the FLAPW with the results from the FSKKR calculations. In the left panel of Fig. 5, we present the DOS of the Mn atom

at the MnSb/In and MnSb/P interfaces together with the bulk FLAPW calculations, while in the right panel of the same figure we present the DOS for the Ni atom at the Ni/P and Ni/In interfaces. We can directly compare these results with the FSKKR results on the same systems shown in the left-top and left-down panels of Fig. 4. Except for very small details, both methods give a similar density of states. In the case of the MnSb/In interface, the Fermi level falls within a local minority minimum while for the MnSb/P interface, due to the smaller exchange splitting, Mn unoccupied minority states move lower in energy crossing the Fermi level. More importantly, both methods describe to the same degree of accuracy the hybridization between the Ni d orbitals and the In or P p states. For the Ni/In contact, the Fermi level is pinned within a minority Ni peak, the only difference being that this peak is larger in the case of the FSKKR calculations. In the case of the Ni/P interface, the minority Ni DOS at the Fermi level is very small, as was the case for the FSKKR results above. Moreover, both methods yield similar spin magnetic moments at the interfaces (and thus the spin moments calculated with the FLAPW method are not presented here).

To make our results more clear, in Fig. 6 we have gathered the layer-resolved partial DOS at the Fermi level for all the (001) interfaces studied with the FLAPW method. As we already mentioned in Sec. II, we have used a slab made up from eight NiMnSb and eight InP layers. Thus if one interface is MnSb/In (shown in the middle of the top figure), then the other interface is Ni/P-like and it consists of the two layers shown at the edges of this figure (the slab is periodically repeated along the axis perpendicular to the interface). Similarly, the bottom graph contains the results for the MnSb/P and Ni/In interfaces. The layers at the middle of the semiconductor spacer show a small DOS due to both the induced states from the half-metal and bulk NiMnSb states which decay slowly outside the half-metallic spacer and travel throughout the semiconductor. It is clearly seen that none of the interfaces is in reality half-metallic. For the MnSb/In interface, the Mn atom at the interface shows an

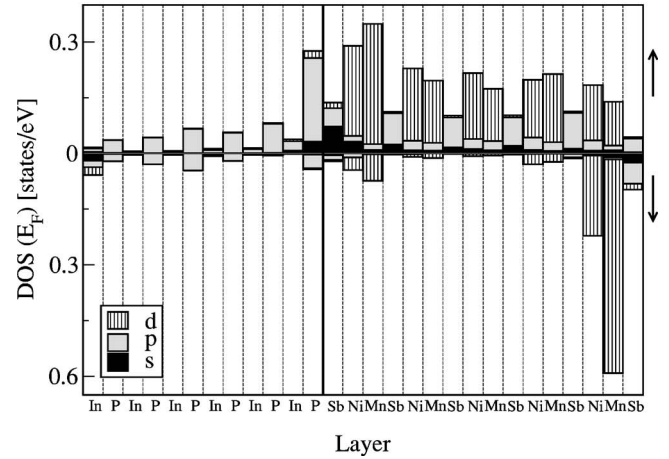
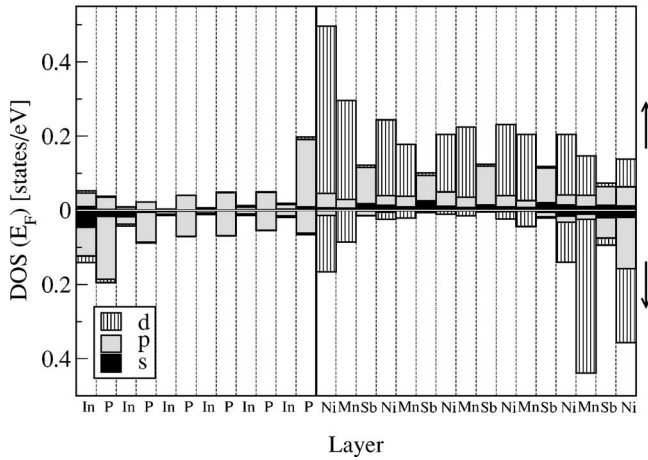
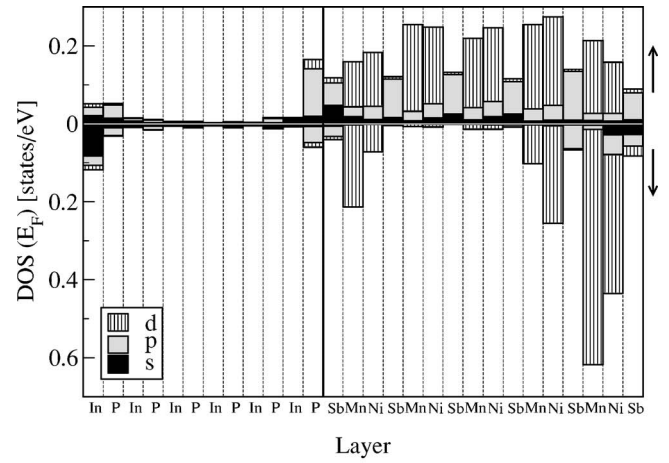
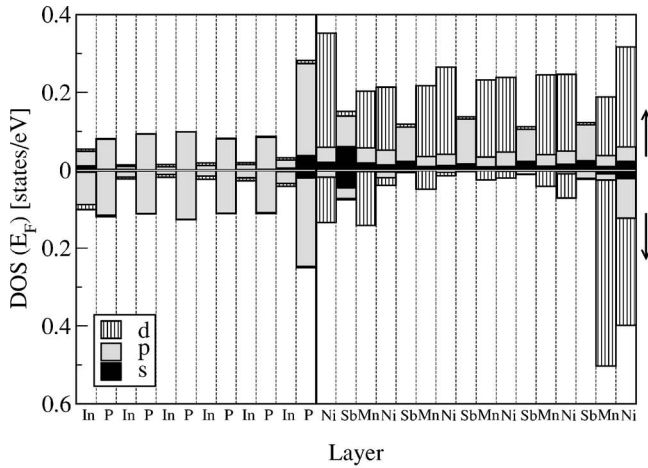


FIG. 7. Layer-resolved DOS at the Fermi level for the Ni-terminated NiMnSb/InP(111) contacts calculated using the FLAPW method. In the middle of the figures, a Ni/P interface is shown with Sb (top) or Mn (bottom) in the subinterface layer, while at the borders of the figures the layers of a Ni/In interface can be seen with Mn (top) or Sb (bottom) in the subinterface layer.

FIG. 8. Layer-resolved DOS at the Fermi level for the Sb-terminated NiMnSb/InP(111) contacts calculated using the FLAPW method. In the middle of the figures, a Sb/P interface is shown with Mn (top) or Ni (bottom) in the subinterface layer, while at the borders of the figures the layers of a Sn/In interface can be seen with Ni (top) or Mn (bottom) in the subinterface layer.

electrons at the Fermi level than majority ones, as can be seen from the DOS at the boundaries of the pictures in Fig. 8.

In Fig. 8, we also show the two different P/Sb-terminated interfaces: In the top panel, the one with Mn as a subinterface layer is not of particular interest since the Mn atom shows a practically zero net spin polarization decreasing considerably the overall spin polarization at the interface. On the other hand, when the subinterface layer is Ni as in the middle of the bottom panel, all atoms at the interface show a very high majority DOS at the Fermi level and the resulting spin polarization, P , is $\sim 74\%$ and thus $\sim 86\%$ of the electrons at the Fermi level are of majority character. We should also mention that, although the induced majority DOS at the Fermi level for the P atom at the interface seems very large (it is of the same order of magnitude with the Ni one), when we move away from the Fermi level it becomes very small compared to the majority DOS of the transition-metal atoms.

The main question that still needs to be answered is why the two different P/Sb interfaces show such large differences. It is mainly the Mn atom whose spin polarization at

the Fermi level is very different depending on its distance from the interface. To answer this question, in Fig. 9 we have gathered the layer-resolved DOS for the two different P/Sb interfaces and in this figure we also included the atomic spin moments. The Sb spin moments are $-0.02\mu_B$ for the $\cdots\text{In}-\text{P}/\text{Sb}-\text{Mn}-\text{Ni}\cdots$ interface and $-0.04\mu_B$ for the $\cdots\text{In}-\text{P}/\text{Sb}-\text{Ni}-\text{Mn}\cdots$ interface. In both cases this is smaller than the bulk value of $-0.06\mu_B$. The Mn spin moment for the $\cdots\text{In}-\text{P}/\text{Sb}-\text{Mn}-\text{Ni}\cdots$ case is $3.72\mu_B$, close to the bulk value of $3.70\mu_B$, considerably larger than the Mn moment of $3.47\mu_B$ for the $\cdots\text{In}-\text{P}/\text{Sb}-\text{Ni}-\text{Mn}\cdots$ case. One would expect that in the first case the exchange splitting should be larger and the unoccupied minority states would be higher in energy but, as can be seen in Fig. 9, the contrary effect occurs. In the second case, the Mn is deeper in the interface and its environment is more bulklike and the minority states are pinned at their position and thus the Fermi level falls within a minority local minimum resulting in a very high spin polarization. At the $\cdots\text{In}-\text{P}/\text{Sb}-\text{Mn}-\text{Ni}\cdots$ contact, the Mn atom is closer to the interface. Here, the larger hybridization of the Mn minority states (not only with the p

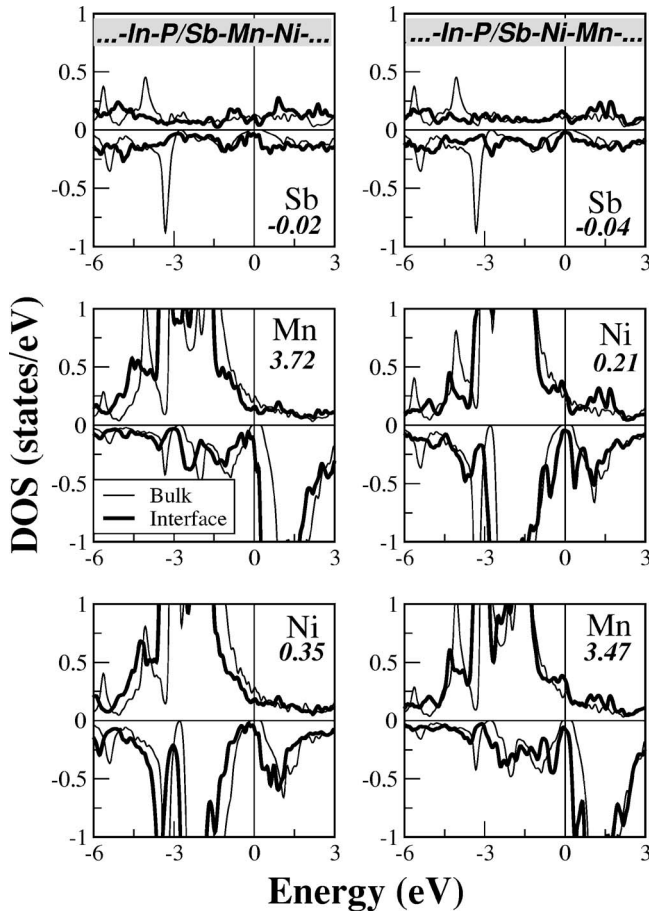


FIG. 9. Atom- and spin-resolved DOS for the $\cdots\text{In-P/Sb-Mn-Ni}\cdots$ interface (left panels) and the $\cdots\text{In-P/Sb-Ni-Mn}\cdots$ interface (right panels) calculated with the FLAPW method. The values in the figures are the spin moments of the atoms at the interface in μ_B . The thin solid line indicates the bulk results.

orbitals of Sb but also with the ones of P, since the last ones are closer now) obliges the minority states to move slightly lower in energy. Thus, the Fermi level does not fall in the local minimum but shifts into the peak of the unoccupied minority states and the net spin polarization vanishes. The Ni states are strongly polarized by the Mn ones, and also in the case of the Ni atom which is deeper than the Mn one, the Fermi level does not fall anymore within the local minimum.

In their paper, Wijs and de Groot predicted that the interfaces between the Sb-terminated NiMnSb(111) film and a S-terminated CdS(111) film should keep the half-metallicity or at least show an almost 100% spin polarization at the Fermi level.²² This is not a contradiction to our results, since Wijs and de Groot considered the case of an interface where the S atoms sit exactly on top of the Sb atoms. As noticed by these authors, a similar structure can also be realized with InP instead of CdS. Therefore, we calculated also an $\cdots\text{In-P/Sb-Ni-Mn}\cdots$ (111) interface, where the P atoms sit exactly on top of Sb. In this case, a long (2.61 Å) Sb—P bond is formed, which—like in the case of CdS—is stable and the half-metallicity at the interface is preserved. Although CdS and InP have the same number of valence electrons, this is a remarkable result, since S and P have one

electron difference and the electrostatics for the two interfaces are slightly different, resulting in a small displacement of the Fermi level. Although our total energy calculations show that this geometry (on-top stacking) is stable with respect to other stacking variants, it is not clear which stacking will be formed under experimental growth conditions, i.e., layer-by-layer growth.

Similarly to the (001) interfaces in Sec. III C, we also calculated the band offset in the case of the (111) interfaces. The band offset ranges from 0.36 eV in the case of the $\cdots\text{In-P/Mn-Sb-Ni}\cdots$ contact up to ≈ 1 eV for the $\cdots\text{In-P/Sb-Ni-Mn}\cdots$ configuration. Thus the conclusions of Sec. III C are valid also for these interfaces. A certain ambiguity in the evaluation of the band offsets is caused by the fact that the inequivalency of the two interfaces induces an electric field in both the bulk sides of the junction, which shows up as a finite slope in the core-level binding energies as a function of the distance from the interface. While this effect is small in the half-metal, due to the poor screening in the semiconductor we observe a pronounced bending on top of this slope in this side of the junction. Nevertheless, the middle of the semiconductor provides a reasonable reference point for the evaluation of the band offsets.

V. SUMMARY AND CONCLUSIONS

In the first part of our study, we investigated the electronic and magnetic properties of the (001) interfaces between the half-metal NiMnSb and the binary semiconductors InP and GaAs using two different full-potential *ab initio* techniques. Both methods gave similar results in the case of the NiMnSb/InP(001) contacts. In all cases, the (001) interfaces lose the half-metallicity but in the case of the Ni/P contact the Ni has a bulklike behavior since the P atoms substitute the cutoff Sb isovalent neighbors and 70% of the electrons are of majority-spin character at the Fermi level. But in the case of the Ni/As interface, the large hybridization at the interface suppresses this high spin polarization. MnSb-terminated interfaces, on the other hand, present very intense interface states which penetrate also into the deeper layers of the NiMnSb film.

We studied the effect of relaxations on a (001) NiMnSb/InP interface. As discussed above, an unrelaxed Ni/P contact shows a quite large spin polarization, reaching 39%. But structural optimization leads to a large contraction between the Ni and P layers and the increased hybridization suppresses the spin polarization, which for the relaxed case reaches then only a value of 17%. Thus, relaxations can seriously decrease the obtained values of spin polarization, but other mechanisms like the alloying with Cu at the interface can reverse this tendency.

In the second part of our study, we investigated all the possible (111) interfaces between NiMnSb and InP. In all cases, interface states destroy the half-metallicity but in two cases the interface presents high spin polarization. First, when the contact is the $\cdots\text{In-P/Ni-Mn-Sb}\cdots$, the Ni atom at the interface has a bulklike environment and the spin polarization at the Fermi level is as high as 53%. In the

case of the $\cdots\text{—In—P/Sb—Ni—Mn—}\cdots$ contact, the spin polarization is even higher, reaching a value of 74%, but when we consider the case where the P atoms sit exactly on top of the Sb ones (similarly to the case studied in Ref. 22), the half-metallicity is conserved.

Although half-metallicity at the interfaces is in general lost, there are few contacts in which a high spin polarization remains, which makes them attractive for realistic applications. Interface states are important because the interaction with defects makes them conducting and lowers the effi-

ciency of devices based on spin injection. Thus, building up interfaces with the highest spin polarization possible like the ones proposed here is a prerequisite but not a guarantee to achieve highly efficient spin injection.

ACKNOWLEDGMENTS

This work was financed in part by the BMBF under the auspices of the Deutsches Elektronen-Synchrotron DESY under Contract No. 05 KSIMPC/4.

*Electronic address: I.Galanakis@fz-juelich.de

- ¹I. Žutić, J. Fabian, and S. Das Sarma, *Rev. Mod. Phys.* **76**, 323 (2004).
- ²O. Wunnicke, Ph. Mavropoulos, R. Zeller, P. H. Dederichs, and D. Gründler, *Phys. Rev. B* **65**, 241306(R) (2002).
- ³Ph. Mavropoulos, O. Wunnicke, and P. H. Dederichs, *Phys. Rev. B* **66**, 024416 (2002).
- ⁴R. A. de Groot, F. M. Mueller, P. G. van Engen, and K. H. J. Buschow, *Phys. Rev. Lett.* **50**, 2024 (1983).
- ⁵E. Kulatov and I. I. Mazin, *J. Phys.: Condens. Matter* **2**, 343 (1990).
- ⁶S. V. Halilov and E. T. Kulatov, *J. Phys.: Condens. Matter* **3**, 6363 (1991).
- ⁷S. J. Youn and B. I. Min, *Phys. Rev. B* **51**, 10 436 (1995).
- ⁸V. N. Antonov, P. M. Oppeneer, A. N. Yaresko, A. Ya. Perlov, and T. Kraft, *Phys. Rev. B* **56**, 13 012 (1997).
- ⁹I. Galanakis, S. Ostanin, M. Alouani, H. Dreyssé, and J. M. Wills, *Phys. Rev. B* **61**, 4093 (2000).
- ¹⁰I. Galanakis, P. H. Dederichs, and N. Papanikolaou, *Phys. Rev. B* **66**, 134428 (2002).
- ¹¹M. M. Kirillova, A. A. Makhnev, E. I. Shreder, V. P. Dyakina, and N. B. Gorina, *Phys. Status Solidi B* **187**, 231 (1995).
- ¹²K. E. H. M. Hanssen, P. E. Mijnders, L. P. L. M. Rabou, and K. H. J. Buschow, *Phys. Rev. B* **42**, 1533 (1990).
- ¹³P. Bach, A. S. Bader, C. Rüster, C. Gould, C. R. Becker, G. Schmidt, L. W. Molenkamp, W. Weigand, C. Kumpf, E. Umbach, R. Urban, G. Woltersdorf, and B. Heinrich, *Appl. Phys. Lett.* **83**, 521 (2003).
- ¹⁴P. Bach, C. Rüster, C. Gould, C. R. Becker, G. Schmidt, and L. W. Molenkamp, *J. Cryst. Growth* **251**, 323 (2003).
- ¹⁵W. van Roy, M. Wojcik, E. Jedryka, S. Nadolski, D. Jalabert, B. Brijs, G. Borghs, and J. De Boeck, *Appl. Phys. Lett.* **83**, 4214 (2003).
- ¹⁶W. van Roy, J. de Boeck, B. Brijs, and G. Borghs, *Appl. Phys. Lett.* **77**, 4190 (2000).
- ¹⁷J.-P. Schlomka, M. Tolan, and W. Press, *Appl. Phys. Lett.* **76**, 2005 (2000).
- ¹⁸D. Ristoiu, J. P. Nozières, C. N. Borca, T. Komesu, H.-K. Jeong, and P. A. Dowben, *Europhys. Lett.* **49**, 624 (2000).
- ¹⁹D. Ristoiu, J. P. Nozières, C. N. Borca, B. Borca, and P. A. Dowben, *Appl. Phys. Lett.* **76**, 2349 (2000).
- ²⁰J. Giapintzakis, C. Grigorescu, A. Klini, A. Manousaki, V. Zorba, J. Androulakis, Z. Viskadourakis, and C. Fotakis, *Appl. Phys. Lett.* **80**, 2716 (2002).
- ²¹S. Gardelis, J. Androulaki, P. Migiakis, J. Giapintzakis, S. K. Clowes, Y. Bugoslavsky, W. R. Branford, Y. Miyoshi, and L. F. Cohen, *J. Appl. Phys.* **95**, 8063 (2004).
- ²²G. A. Wijs and R. A. de Groot, *Phys. Rev. B* **64**, 020402(R) (2001).
- ²³A. Debernardi, M. Peressi, and A. Baldereschi, *Mater. Sci. Eng., C* **23**, 743 (2003).
- ²⁴S. Picozzi, A. Continenza, and A. J. Freeman, *J. Appl. Phys.* **94**, 4723 (2003).
- ²⁵S. Picozzi, A. Continenza, and A. J. Freeman, *J. Phys. Chem. Solids* **64**, 1697 (2003).
- ²⁶I. Galanakis, *J. Phys.: Condens. Matter* **16**, 8007 (2004).
- ²⁷Ph. Mavropoulos, K. Sato, R. Zeller, P. H. Dederichs, V. Popescu, and H. Ebert, *Phys. Rev. B* **69**, 054424 (2004).
- ²⁸Ph. Mavropoulos, I. Galanakis, V. Popescu, and P. H. Dederichs, *J. Phys.: Condens. Matter* **16**, S5759 (2004).
- ²⁹I. Galanakis, *Phys. Rev. B* **71**, 012413 (2005).
- ³⁰G. Schmidt, D. Ferrand, L. W. Molenkamp, A. T. Filip, and B. J. van Wees, *Phys. Rev. B* **62**, R4790 (2000).
- ³¹G. Schmidt, C. Gould, P. Grabs, A. M. Lunde, G. Richter, A. Slobodskyy, and L. W. Molenkamp, *Phys. Rev. Lett.* **92**, 226602 (2004).
- ³²R. Zeller, P. H. Dederichs, B. Újfalussy, L. Szunyogh, and P. Weinberger, *Phys. Rev. B* **52**, 8807 (1995).
- ³³N. Papanikolaou, R. Zeller, and P. H. Dederichs, *J. Phys.: Condens. Matter* **14**, 2799 (2002).
- ³⁴S. H. Vosko, L. Wilk, and N. Nusair, *Can. J. Phys.* **58**, 1200 (1980).
- ³⁵P. Hohenberg and W. Kohn, *Phys. Rev.* **136**, B864 (1964).
- ³⁶W. Kohn and L. J. Sham, *Phys. Rev.* **140**, A1133 (1965).
- ³⁷R. Zeller, *J. Phys.: Condens. Matter* **16**, 6453 (2004).
- ³⁸E. Wimmer, H. Krakauer, M. Weinert, and A. J. Freeman, *Phys. Rev. B* **24**, 864 (1981).
- ³⁹M. Weinert, E. Wimmer, and A. J. Freeman, *Phys. Rev. B* **26**, 4571 (1982).
- ⁴⁰<http://www.flapw.de>
- ⁴¹I. Galanakis, P. H. Dederichs, and N. Papanikolaou, *Phys. Rev. B* **66**, 174429 (2002).
- ⁴²J. P. Perdew, K. Burke, and M. Ernzerhof, *Phys. Rev. Lett.* **77**, 3865 (1996).
- ⁴³I. Galanakis, *J. Phys.: Condens. Matter* **14**, 6329 (2002).
- ⁴⁴I. Galanakis, *J. Magn. Magn. Mater.* **288**, 411 (2005).
- ⁴⁵S. J. Jenkins and D. A. King, *Surf. Sci.* **494**, L793 (2001).
- ⁴⁶M. Lezaic, I. Galanakis, G. Bihlmayer, and S. Blügel, *J. Phys.: Condens. Matter* **17**, 3121 (2005).
- ⁴⁷S. Massidda, B. I. Min, and A. J. Freeman, *Phys. Rev. B* **35**, 9871 (1987).